Icarus **145**, 33–43 (2000)
doi:10.1006/icar.2000.6339, available online at http://www.idealibrary.com on IDEAL®

Earth Trojan Asteroids: A Study in Support of Observational Searches

Paul Wiegert and Kimmo Innanen

Department of Physics and Astronomy, York University, Toronto, Ontario M3J 1P3, Canada; and CITA, University of Toronto, Toronto, Ontario M5S 3H8, Canada
E-mail: wiegert@yorku.ca

and

Seppo Mikkola

Tuorla Observatory, University of Turku, 21500 Piikkiö, Finland

Received April 13, 1999; revised December 10, 1999

Observational searches for asteroids orbiting near Earth's triangular Lagrange points face unique obstacles. A population of such asteroids would occupy a large projected area on the sky (possibly hundreds of square degrees) and is not favorably placed with respect to the Sun. Here we examine the properties of synthetic populations of Earth "Trojans" in order to aid in the optimization of observational searches for them. We find that the highest on-sky projected number densities are not located at the positions of the L_4 and L_5 points themselves, but rather a few degrees closer to the Sun. Also, asteroids on orbits about the L_4 and L_5 points typically brighten as the difference between their ecliptic longitude and that of the Sun increases owing to phase effects, but their number density on the sky concurrently falls rapidly.

Key Words: **asteroids, dynamics; Earth; resonances.**

1. INTRODUCTION

General analytical solutions to the gravitational three-body problem do not exist; however, certain special solutions do. Perhaps the best known is the classical work of J. L. Lagrange. Given a primary M with a secondary $m \ll M$ in a circular orbit around it, he deduced that there were five points in the system at which a massless particle could, in a frame corotating with the secondary, remain stationary indefinitely. These solutions are commonly known as the Lagrange points. Lagrange's computations are not strictly valid for the case of a planet orbiting in our own, more complex Solar System; nevertheless these solutions retain much importance. Of particular interest here are the "tadpole" orbits that particles may move along in the vicinity of the two so-called "triangular" Lagrange points for the case where the relative orbit of M and m is nearly circular. These two L points are located at the vertices of the two equilateral triangles that can be drawn in the secondary's orbital plane with the primary–secondary line as one side. The leading point is usually called L_4, the trailing, L_5. A more detailed treatment of this subject can be found in Szebehely (1967).

Lagrange's solutions went from the realm of theoretical curiosities to reality with the discovery in 1906 of asteroid 588 Achilles, associated with the L_4 point of the Jupiter–Sun system (Pilcher 1979). Since then, many more "Trojan" asteroids have been found. At this writing, the Minor Planet Center lists 466 asteroids at the L_4 and L_5 points of Jupiter and two for Mars (5261 Eureka and 1998 VF31), but as yet none has been detected near the corresponding points of any other planet. The recent discovery (Wiegert *et al.* 1997) that asteroid 3753 Cruithne is in a $1:1$ coorbital resonance (though not a "Trojan" one) with Earth encourages a revisit of the question of whether Earth has other co-orbital companions. In this paper, we examine the properties of synthetic populations of asteroids orbiting about the L_4 and L_5 points of Earth, for the purpose of aiding in future observational searches. We do not investigate the origin or stability of such objects here, but will rather assume some population of objects on such orbits, and ask how best to detect them.

We do, however, note that the Earth/Sun mass ratio is sufficiently small for the triangular Lagrange points to be at least linearly stable in the three-body context (Danby 1964). Extensive investigations of the stability of the triangular Lagrange points have been performed by many authors, though relatively few have considered whether Earth in particular can maintain a population of such bodies. However, at least certain Earth Trojan asteroid (ETA) orbits have been found (numerically) to be stable against perturbations from the other planets in the Solar System for times up to 10^5 yr (Weissman and Wetherill 1974, Dunbar 1980, Mikkola and Innanen 1990). Mikkola and Innanen (1995) studied a population of ETAs over somewhat longer time scales (10^6–10^7 yr) and found instabilities at inclinations in the range of 10°–25°. Such time spans fall far short of the 4.5×10^9 yr age of the Solar System. Nevertheless, even if ETA orbits prove unstable on longer time scales, captured

0019-1035/00 $35.00

near-Earth asteroids may provide a transient population of such objects.

Current telescopes and detectors should easily be able to detect ETAs, their proximity to both Earth and the Sun making them relatively bright. However, searches for such objects are not without their difficulties. The nearness of these bodies to Earth means that any Trojan group would cover a large projected area on the sky; we will see in Section 3.1 that such a cloud may extend over hundreds of square degrees with only a very broad central peak. As well, the necessary proximity of these asteroids to the triangular Lagrange points requires observations to be made in the morning and evening, and hence subject to higher airmasses and the increased sky brightness of twilight. Observational searches for ETAs thus present interesting challenges.

One strategy useful for the detection of faint moving bodies involves tracking the telescope at the expected apparent angular velocity $\dot{\theta}$ of the object in question. This results in the searched-for object's image remaining stationary upon the detector and building up its signal, while objects moving at different speeds (e.g., stars) can be excluded by their streak-like appearance. For this reason, the apparent angular velocity of ETAs is examined here. One should note that the angular velocity of an object located at either triangular Lagrange point is not zero. Though the L points are stationary with respect to the Earth–Sun line (i.e., in the frame which corotates with the Earth), they complete a full circuit against the background stars every year and hence their mean relative angular rate should be $\dot{\theta} \approx 150''/\mathrm{h}$.

The most recent search for Earth Trojan asteroids was performed by Whiteley and Tholen (1998), who were able to cover 0.35 square degrees close to the classical L_4 and L_5 points down to $R \sim 22.8$ using CCD detectors. In that paper, they also provide many additional, valuable insights affecting current search strategies. Their paper served as a primary motivation for our work. An earlier photographic search was performed by Dunbar and Helin (1983), also without detections but putting a limit of 7 ± 3.5 objects with visual absolute magnitudes brighter than 20 "in the L_4 region." Unfortunately, they do not report how many square degrees of the sky they sampled with the 18 plates they obtained. It is likely to be much less than the extent of the hypothetical Trojan clouds presented here, but in any case, the missing information makes a comparison with other results impossible.

Though the absence of detections may indicate an absence of ETAs, searches to date have likely only sampled a relatively small portion of the potential Trojan cloud, and we will see in Section 3 that the existence of a population of Earth Trojans cannot be rejected at this time.

Our model is presented in Section 2; the results are discussed in Section 3 and our conclusions are presented in Section 4.

2. MODEL CALCULATIONS

In order to determine how best to detect a population of Earth Trojans, something must first be known about their properties. Studies of main-belt and near-Earth asteroids allow us to make estimates of ETA albedos and other surface properties. Estimating their spatial distribution is less straightforward, but our knowledge of the jovian Trojan group and current numerical models of the Solar System should provide us with a reasonable starting place.

We examine two synthetic populations of Earth Trojans. Both have semi-major axes chosen uniformly and randomly in the coorbital region between the L_1 and L_2 points, i.e., $0.997 \le a \le 1.003$ AU, based on the stability limits for Earth Trojans found by Weissman and Wetherill (1974). The width of this zone matches the width of the resonance overlap zone predicted by the $\mu^{2/7}$ law (Wisdom 1980, Duncan *et al.* 1989, Murray and Holman 1998). This relation states that if a is the semi-major axis of a planet and μ is the ratio of its mass to the total (i.e., planet plus Sun), then small bodies with semi-major axes differing from a by $\Delta a \gtrsim \mu^{2/7}$ are isolated from the 1 : 1 resonance by a region of quasi-periodic (i.e., nonchaotic) trajectories. The $\mu^{2/7}$ law thus defines a boundary beyond which a simulated test body has effectively escaped from 1 : 1 resonance.

Apart from the value of the semi-major axis, the first (or "broad") population is given orbital elements that are chosen based on the breadth of the distribution of Jupiter's Trojans, as listed on the Minor Planet Center's Web site (http://cfa-www.harvard.edu/iau/lists/Trojans.html). The eccentricities e and inclinations i are chosen randomly from the uniform distributions $0 \le e \le 0.3$ and $0^\circ \le i \le 30^\circ$. A random longitude of the ascending node Ω and argument of perihelion ω is assigned to each particle, and its mean anomaly chosen such that its mean longitude is either 60° ahead of or behind the Earth.

A second (or "narrow") population is also examined, its element distributions based on the locations of the peaks in the orbital element distributions of Jupiter's Trojans. In this case, the eccentricity and inclination are chosen from $0 \le e \le 0.1$ and $0^\circ \le i \le 10^\circ$ instead.

The particle populations chosen are then integrated for 10^5 yr with a Wisdom–Holman (Wisdom and Holman 1991) integrator using a 3-day time step in a Solar System including all the planets except Pluto. Those particles which remain on Trojan (or tadpole) orbits throughout the entire integration (i.e., those whose longitude relative to Earth remains consistently either ahead of or behind our planet) will be considered our sample. This integration interval allows the removal of objects that do not remain on Trojan orbits (with the tacit assumption that such short-lived objects do not constitute an appreciable fraction of the Earth Trojan population). Of the broad population, 63 of 100 initial conditions pass this criterion (primarily those at low e); 95 of 100 of the narrow population's members do. We have also performed 10^6-yr integrations for the trailing Lagrange point with little change in the survival fraction or other results.

We have deliberately chosen to exclude horseshoe orbits from this study, though asteroid 3753 Cruithne (Wiegert *et al.* 1997) is proof that bodies on non-tadpole 1 : 1 mean motion resonances exist. Nevertheless, the apparent lack of such a population for

Jupiter has lead us to examine the possible traditional Trojan population first, though a similar study for possible horseshoe orbits would also be of interest.

During the simulations, the eccentricities and inclinations of the particles are monitored. Various perturbations induce oscillations in these quantities, but their amplitudes are rather small. For the eccentricity, e is found to vary by ± 0.01 near $e = 0$ up to ± 0.025 at $e \gtrsim 0.2$. The inclination varies typically by $\pm 3^\circ$. All of e, i, and ω show these oscillations with periods of 10^4–10^5 yr, typical of secular perturbations by the giant planets. The longitude of the node varies on much shorter time scales (10^2 yr), most likely driven by close encounters with the planet, which have a similar time scale.

In addition to the orbital elements, the apparent geocentric position and other properties (phase, apparent magnitude, etc.) are measured at regular (but noncommensurable) intervals. This set of synthetic "observations" should provide a benchmark with which to optimize observing strategies.

The apparent visual magnitude of our simulated asteroids is calculated using the IAU two-parameter magnitude relation (Bowell *et al.* 1989), which we will term $M_V(r_\odot, r_\oplus, \alpha, H, G)$; $r_\odot$ is the asteroid–Sun distance, $r_\oplus$ is the asteroid–Earth distance, and α is the phase angle, i.e., the angle between the Sun and Earth as seen from the asteroid. The two parameters in question are the absolute magnitude H of the asteroid, and G, the so-called "slope parameter," which describes the change in brightness with phase. These parameters depend on the particular properties of a given asteroid, and thus are unknown for our sample. However, since apparent magnitude scales linearly with H, we simply calculate the difference between the apparent and absolute magnitude, which we will call the magnitude adjustment ΔM_V, defined such that

$$\Delta M_V(r_\odot, r_\oplus, \alpha, G) = M_V(r_\odot, r_\oplus, \alpha, H, G) - H. \quad (1)$$

The G factor has a relatively weak influence on apparent magnitude, and we simply adopt a value of 0.15, noting that the most common asteroids have typical G values ranging from 0.1 (C type) to 0.25 (S type) (Bowell *et al.* 1989, Piironen *et al.* 1997). Note that no albedo or diameter need be assumed, these unknowns being subsumed into the absolute magnitude H.

The detection of faint ETAs will be hampered by the presence of crowded star fields; in particular, the positions of the Lagrange points relative to the Milky Way should be considered. This issue was addressed by Whiteley and Tholen (1998), and we simply quote it here for completeness. The L_4 point is at its highest galactic latitudes during April through June and October through December, the L_5 point during December through February and June through August.

Asteroids orbiting both the leading and trailing triangular Lagrange points have been studied. The populations of these two regions, should they exist, may differ (e.g., the leading/trailing ratio for Jupiter Trojans is $292/176 \approx 1.66$, though observational biases complicate this picture), but our dynamical simulations, as yet, give no hint of such a possible skew. In both leading and trailing cases, almost the same fraction of the ETAs (63 and 95% for the broad and narrow populations, respectively) remain on tadpole orbits for the full 10^5-yr integration, and the resulting distributions of elements, positions, etc., are very similar, though the randomized initial conditions ensure that the leading and trailing distributions are not identical. In the interests of brevity, we will discuss here only the trailing distribution, with the afore-mentioned caveat in mind.

Three questions will spearhead our examination of our simulated Earth Trojan population. First, where is the greatest projected density of ETAs on the sky? Second, where are ETAs at their brightest as seen from Earth? And third, which ETAs can be observed under the darkest skies?

3. RESULTS

3.1. Overall Sample

Let the geocentric ecliptic latitude of an ETA at any given time be β, and let the ecliptic longitude relative to the Sun be ℓ. Then, the Sun is always at $\beta = 0^\circ$, $\ell = 0^\circ$. Figure 1 displays the distribution of simulated observations (as described above) against the axes of β and ℓ for both the broad and narrow populations. On this and on the following plots, the darker pixels indicate those at which more synthetic observations were made, while the lighter ones indicate a relative absence.[1] The contours are labeled according to the total number of observations interior to them, and account for the (usually small) number of data points outside the presented frame. Thus the contour labeled "10" is that interior to which the most densely packed 10% of the observations fall; similarly, the "25" contour includes 25% of all observations, and so on. Various statistics of the ETA distributions are presented in Table I.

The plots were subjected to a 3×3 boxcar filter to smooth the contours. The (presmoothing) noise-related uncertainty in each pixel is small in the most heavily populated regions of the graph, with typical peak values of 200 counts, a noise level of roughly 7%. However, the observations are not all independent (and thus not strictly Poissonian in their noise characteristics), belonging to the trajectories of only $\sim$100 test particles and thus effectively increasing the uncertainty in the results. This, together with the assumptions made about the ETAs orbital elements, implies that small-scale structures in the figures must be interpreted with particular caution. Indeed here we will examine only the broad features of these distributions. The one exception we make is to present a magnified view of the peak of the on-sky distribution. Frames (a) and (b) of Figure 1 might conceal a narrow central peak or similar feature of observational interest. However, the high-magnification frames (c) and (d) make it clear that there is no particularly overdense region in the vicinity of the Lagrange

[1] Note: pixel counts are not weighted by apparent brightness; thus these plots are not strictly comparable to long-time exposure "images."

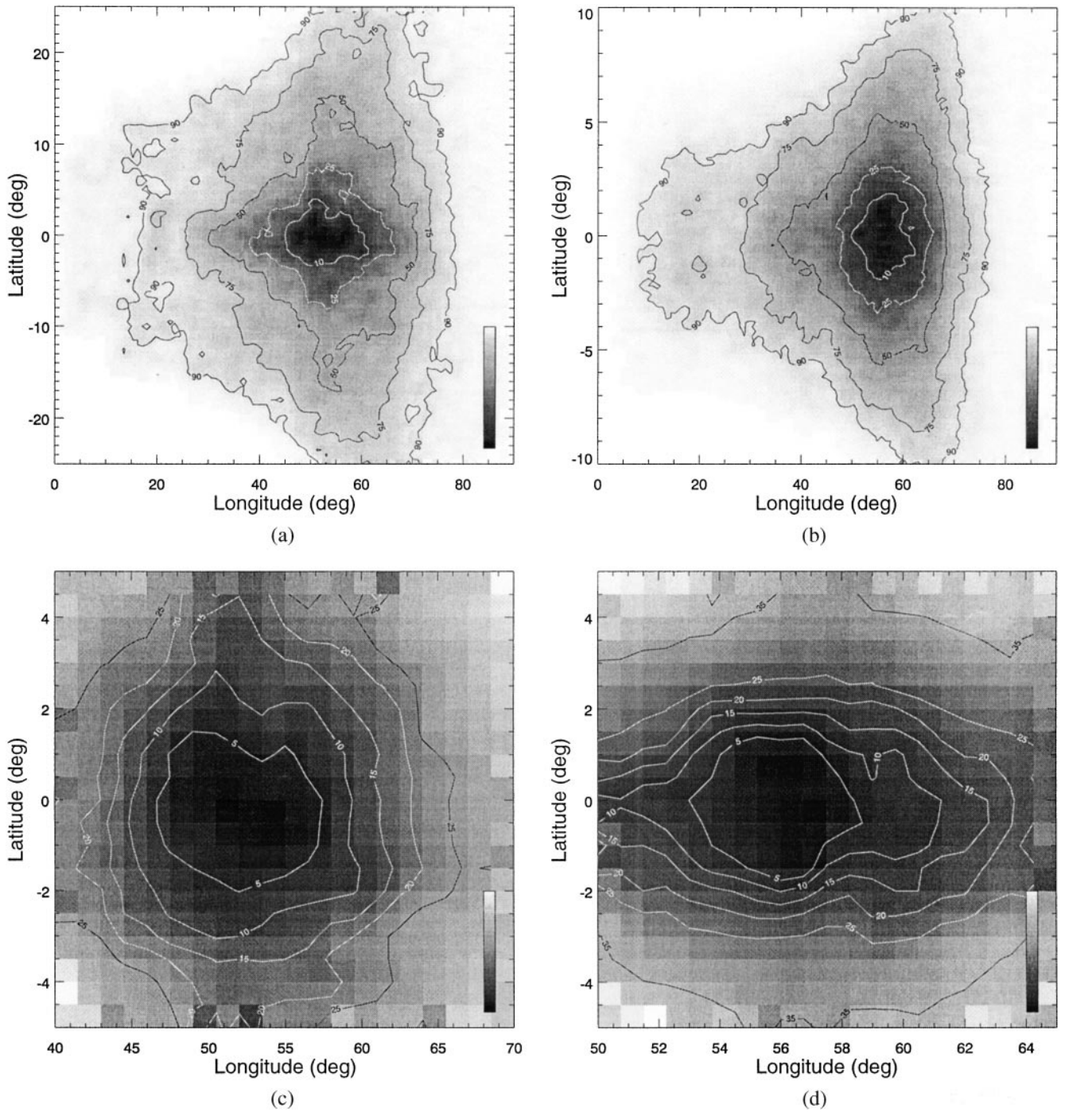

FIG. 1. The distribution of simulated observations plotted against ecliptic latitude and longitude at low (a, b) and high (c, d) magnifications. Black indicates the highest number density, white the lowest. The left-hand figures are for the broad population, the right-hand ones for the narrow. The detail in the low- and high-magnification graphs differ owing to the different binning and smoothing.

points. The reader should note that the details of the contours at low and high magnifications differ somewhat owing to the different binning, which also affects the smoothing algorithm. Both Figs. 1c and 1d have peak pixel values ∼100 (RMS noise ∼10%).

Figure 1 makes clear one of the key difficulties facing ETA searchers: the wide area of sky to be searched. As an illustration, the 10% contour, though it encompasses roughly 60 and 25 square degrees for the broad and narrow populations, respectively, is only occupied by 10% of the ETA population at any given time. Whiteley and Tholen (1998) placed an upper limit of three objects larger than a few hundred meters per square degree in the vicinity of the L_4 and L_5 points. Assuming the 10%

TABLE I
Statistics of the Broad and Narrow Simulated Earth Trojan Populations

	Broad				Narrow			
	Min.	Max.	Med.	Mean	Min.	Max.	Med.	Mean
Ecl. latitude (°)	−85	79	0.0	0.0	−26	26	0.0	0.0
Ecl. longitude (°)	2	126	54	53	4	90	56	53
Mag. adjustment (mag)	−0.6	3.1	2.2	2.2	0.1	2.8	2.3	2.2
Phase (°)	3	120	55	53	5	92	56	53
Dist. from Earth (AU)	0.2	2.1	1.1	1.2	0.3	2.1	1.1	1.2
Angular vel. (″/h)	71	430	147	148	116	209	148	148

contour is populated at this level, 75–180 objects this size could be in this region at any instant. Thus, though past searches in this region have failed to discover such asteroids, the existence of ETAs is still far from being ruled out.

The distribution of simulated ETAs is centered on zero ecliptic latitude, expected from the symmetric distribution of the inclinations and the uniform distribution of the other angular elements. It is highest within a degree or two of the ecliptic plane and has a much broader distribution along the ecliptic.

One should note, however, that the centroid of the highest density contour is not at 60° longitude, i.e., not in the direction of the Lagrange point. Rather the centroid is slightly interior to this point at $\ell \sim 55°$. Since a constant distribution of asteroids along Earth's orbit would remain constant when projected onto the sky, we conclude that the displacement of the centroid is primarily due to the asteroids spending more time in the elongated "tail" of the tadpole, rather than to purely geometrical projection effects. The density variation between 55° and 60° is weak (∼25%) and would make little difference to a survey which could sample only a small area (e.g., less than 1 sq. degree). Nevertheless, this factor should be taken into account when wide-field surveys are attempted.

Figure 2 presents the distribution of the simulated asteroids' apparent magnitude adjustment ΔM_V versus ecliptic latitude and longitude. Asteroids near the projected positions of the Lagrange points are typically 2 to 2.5 magnitudes fainter than their absolute magnitude; e.g., a 6-km-diameter C-type asteroid ($H \approx 15$, Bowell and Lumme 1979, Rabinowitz 1993) would have an apparent magnitude $M_V \approx 17$–17.5. If ETAs have a size distribution similar to that of NEAs (e.g., $N(H) \propto e^{0.9H}$, Rabinowitz 1994) then, given that current limits allow a population of perhaps 10^3 objects with diameters greater than 100 meters ($H \approx 23$), one might expect ∼10 objects in the 5-km range. Of course, such numbers are based on rather loose upper limits, but the existence of kilometer-sized ETAs cannot yet be ruled out. Such objects would certainly be detectable by modern facilities, though again questions of sky brightnesses and tracking rates complicate the issue significantly.

The brightest simulated observations are outside the plot area of Figs. 2a and b. The distribution continues up to brighter magnitudes at ecliptic longitudes near 90°, though at very low number densities. These brightest data points are caused by objects passing very close to Earth. Asteroids near to, but slightly outside Earth's orbit, have their brightness enhanced both by their proximity and their low phase angle. These brightest observations will be discussed in more detail in Section 3.2.

Figure 3 examines the distributions of magnitude versus angular velocity $\dot{\theta}$. The ETAs cluster around 150″/h, but with significant scatter: only 25 and 50% of the broad and narrow populations respectively have $140''/\text{h} < \dot{\theta} < 160''/\text{h}$. Figure 3 also displays the components of $\dot{\theta}$ both parallel (XY) and perpendicular (Z) to the ecliptic. The XY component is centered on $\dot{\theta} \approx 150''/\text{h}$, that being the angular velocity of the Lagrange points. The Z component, which can be significant, is a result of the inclinations of the assumed ETAs. We concur with Whiteley and Tholen (1998) that tracking the telescope at at rate of 150″/h

TABLE II
Statistics of the Brightest ($\Delta M_V < 1.5$) Members of the Simulated Earth Trojan Populations

	Broad				Narrow			
	Min.	Max.	Med.	Mean	Min.	Max.	Med.	Mean
Ecl. latitude (°)	−85	79	−0.3	−1.0	−26	26	−0.1	−0.2
Ecl. longitude (°)	29	126	72	73	61	90	74	74
Mag. adjustment (mag)	−0.6	1.5	1.3	1.2	0.1	1.5	1.3	1.2
Phase (°)	54	113	74	75	63	92	75	74
Dist. from Earth (AU)	0.2	0.65	0.55	0.53	0.3	0.65	0.55	0.54
Angular vel. (″/h)	71	430	166	169	121	209	154	155

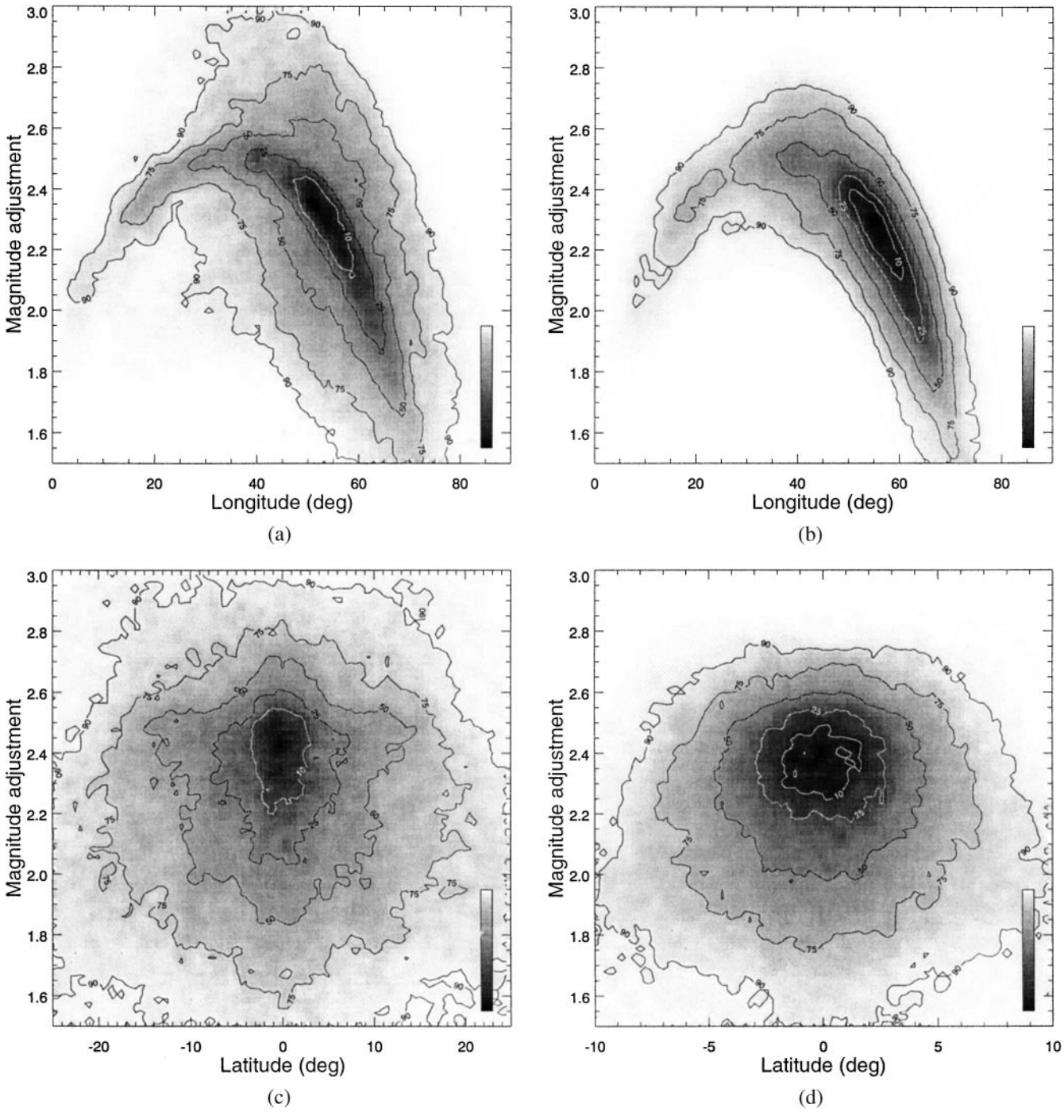

FIG. 2. The distribution of simulated observations plotted against apparent magnitude adjustment and ecliptic longitude (a, b) or latitude (c, d). The left-hand figures are for the broad population, the right-hand ones for the narrow. The magnitude adjustment is defined in Eq. (1).

along the ecliptic is appropriate but will reduce one's sensitivity to high-i objects.

We should point out that non-Trojan near-Earth asteroids could pass through the regions of the sky considered here with apparent motions similar to those of Trojans. Orbital determinations would thus be necessary to confirm the nature of any such detections made.

3.2. Brightest Observations

The brightest ETAs have an obvious advantage for detection. Here we will define the sample of the brightest ETA observations as those with $\Delta M_V < 1.5$. Roughly 5% of the simulated observations fall into this category. Figure 4 presents their distribution on the sky and versus magnitude and apparent angular

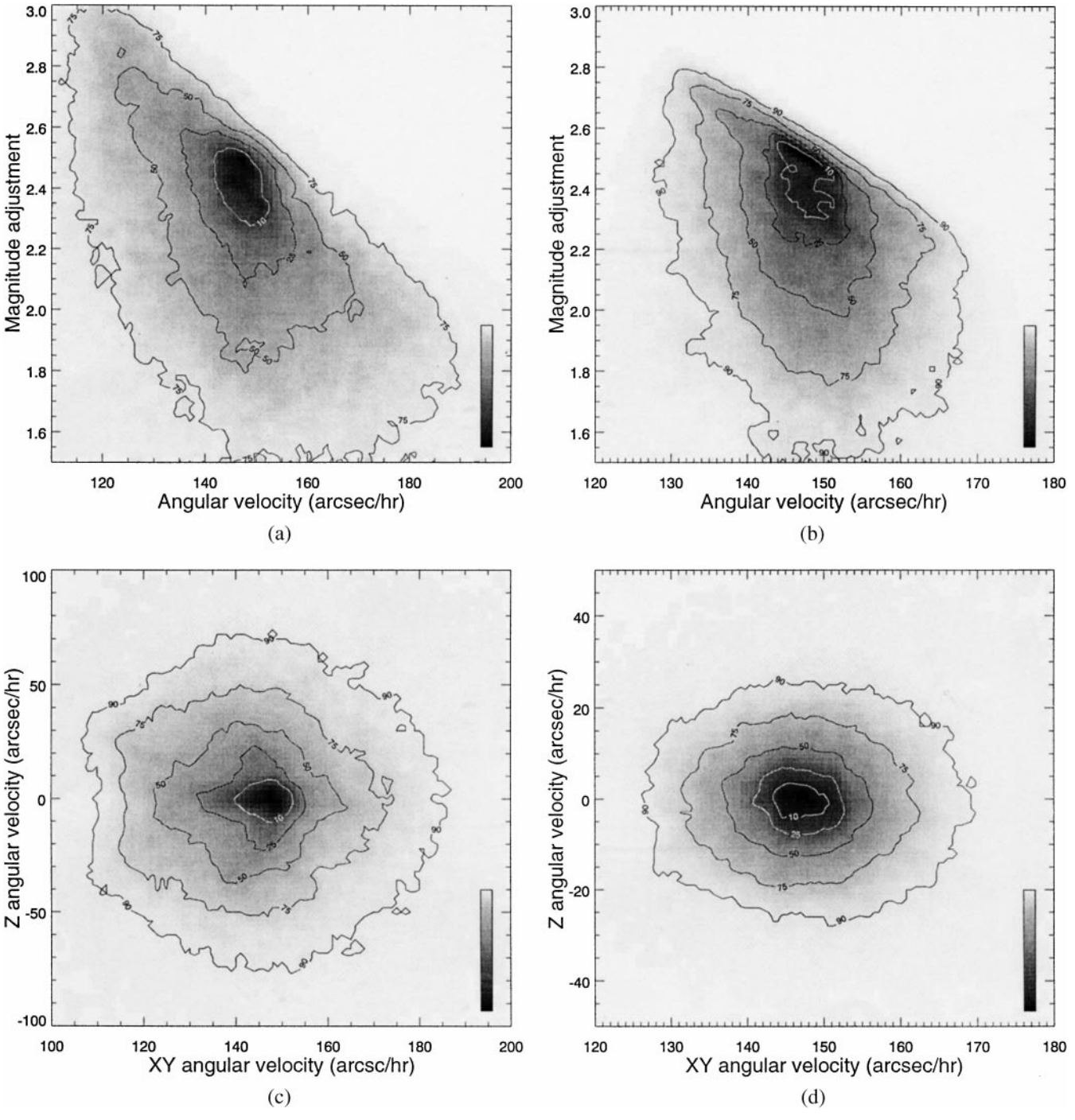

FIG. 3. The distribution of simulated observations plotted against apparent magnitude adjustment and angular velocity (a, b). Figures (c) and (d) show the components of the angular velocity parallel and perpendicular to the ecliptic. The left-hand figures are for the broad population, the right-hand ones for the narrow.

velocity. Some general statistics of the brightest observations are listed in Table II.

The brightest simulated observations are found to be clustered somewhat differently than the general sample. The brightest observations tend to occur nearer to Earth, both because of the $1/r^2$ effect and because of decreased phase angles for bodies outside Earth's orbit. The proximity of these observations to us results occasionally in high ecliptic latitudes (up to $\beta \gtrsim \pm 80^\circ$ for the broad population). The increased brightness resulting from decreased phase angle favors asteroids with positions outside

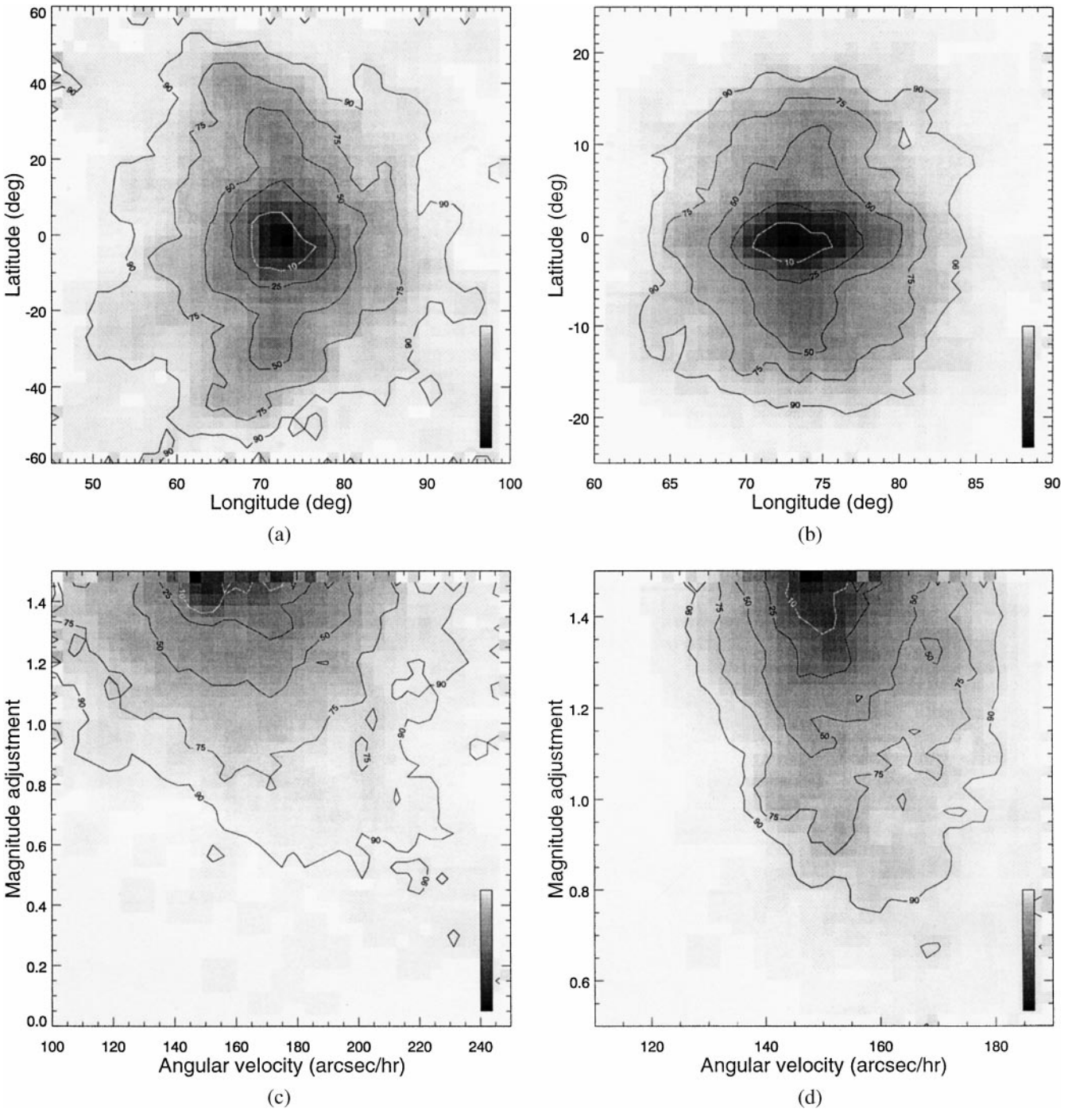

FIG. 4. The brightest simulated observations ($\Delta M_V \leq 1.5$) plotted versus ecliptic latitude and longitude (a, b) and versus magnitude adjustment and angular velocity (c, d). The left-hand figures are for the broad population, the right-hand ones for the narrow. Note that the contours are labeled for the fraction of the population of brightest objects they contain, not the fraction of the total population.

Earth's orbit, and results in a shift of the center of the on-sky distribution to larger ecliptic longitudes. The sample of the brightest observations, as defined above, clusters at $\ell \gtrsim 72^\circ$, but this particular longitude value is an artifact of our choice of cutoff in ΔM_V and the brightening trend for the observations at high ℓ (i.e., low phase). Had we chosen $\Delta M_V \leq 1$ or ≤ 2, we would have found the distribution clustered around 78° or 65°, respectively, instead.

We conclude that searches for ETAs at high ecliptic longitudes are aided by the brightening of the asteroids (and the darker skies available), though at a significant cost in on-sky number density.

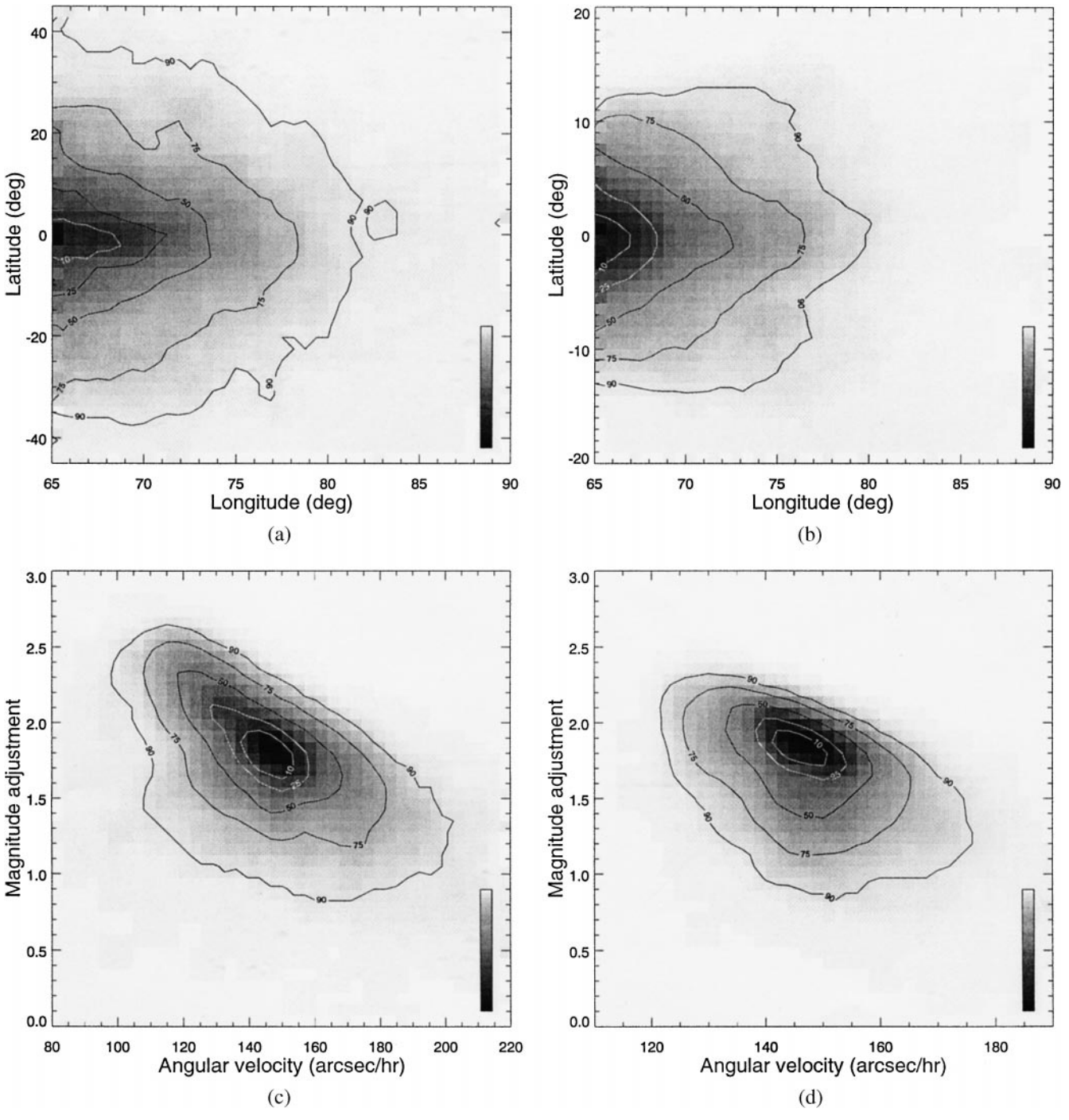

FIG. 5. The simulated observations with the largest ecliptic longitudes ($\ell \geq 65°$) plotted versus ecliptic latitude and longitude (a, b) and versus magnitude adjustment and angular velocity (c, d). The left-hand figures are for the broad population, the right-hand ones for the narrow. Note that the contours are labeled for the fraction of the population of large longitude objects they contain, not the fraction of the total population.

3.3. Large Ecliptic Longitudes

Astronomical observations of objects as faint as ETAs require reasonably dark skies. However, by virtue of their position relative to the Earth–Sun line, the Lagrange points cross the meridian in the daytime. Of course, observations can be obtained of these regions in the evenings and mornings, but are hampered by twilight and high airmasses.

The difference between the right ascension of the Sun and the object in question provides a measure on the time between the

TABLE III
Statistics of the Members of the Simulated Earth Trojan Populations with the Greatest Longitudes ($\ell \geq 65^\circ$)

	Broad				Narrow			
	Min.	Max.	Med.	Mean	Min.	Max.	Med.	Mean
Ecl. latitude (°)	−80	79	−0.23	−0.14	−26	26	0.0	0.0
Ecl. longitude (°)	65	126	70	71	65	90	69	70
Mag. adjustment (mag)	−0.6	2.7	1.8	1.8	0.1	2.4	1.8	1.7
Phase (°)	48	97	65	65	63	92	75	74
Dist. from Earth (AU)	0.2	1.22	0.76	0.76	0.29	1.1	0.75	0.73
Angular vel. (″/h)	82	407	146	148	116	209	147	148

setting and rising of the two. However, RA is a function of the angle between the Earth–Sun line and Earth's axis, and thus a function of the time of year. The question of observability is also affected by the position on the globe of the observatory.

Instead of performing a detailed examination of observability for particular observatories over the course of a year, we use a cruder and more general criterion for determining simulated observations observability. We take the ecliptic longitude difference ℓ of an ETA as a measure of the object's apparent distance from the Sun (i.e., we take Earth's obliquity to be zero). The solar elongation (i.e., the angle between the Sun and the object as seen from Earth) is not a suitable measure here, for we are interested primarily in the Sun–asteroid angular separation when projected on the ecliptic.

We examine the set of ETA observations with longitude differences $\ell \geq 65^\circ$. Roughly 18% of our data points fall into this category, for both broad and narrow populations. The results are displayed in Fig. 5 and Table III. Though scattered observations extend out beyond 120° longitude, only ∼1% of observations for each population are at $\ell > 80^\circ$. These data points are typically brighter than average owing to the decreased phase angle at high longitude, reflected in Table III by a $\Delta M_V \approx 1.8$, compared to 2.2 for the sample as a whole (Table I).

4. CONCLUSIONS

We have examined two hypothetical populations of Earth Trojan asteroids with an eye to clarifying the observational strategies necessary to detect them efficiently. Synthetic observations of an ETA cloud are clustered around the triangular Lagrange points, as expected, and may cover hundreds of square degrees of sky. As a result, current observational limits still allow populations of Earth Trojans of several hundred objects larger than a few hundred meters in size.

However, pointing one's telescope directly toward one of Earth's Lagrange points does not result in an optimal search of the region of the sky most heavily populated by ETAs. In fact, a slightly higher concentration can be found at smaller ecliptic longitude difference $\ell \approx 55^\circ$. Also, there is a trend for ETAs to brighten as ℓ increases due to the decreasing phase angle, and searches also benefit from the darker skies these positions allow. However, the density of objects decreases sharply with ℓ. Thus, observational searches should perhaps be tailored to optimize the local strengths, be they wide field of view or faint limiting magnitude.

ACKNOWLEDGMENTS

We gratefully thank D. Tholen and R. Whiteley for helpful comments, and S. J. Bus and an anonymous referee for their valuable insights. This work was performed while P.W. was a National Fellow at the Canadian Institute for Theoretical Astrophysics, and was supported in part by the Natural Sciences and Engineering Research Council of Canada. K.I. expresses his thanks to Professor Mauri Valtonen of the Tuorla Observatory for his traditional generous hospitality during the preparation of this manuscript.

REFERENCES

Bowell, E., and K. Lumme 1979. Colorimetry and magnitudes of asteroids. In *Asteroids* (T. Gehrels, Ed.), pp. 132–169. Univ. of Arizona Press, Tucson.

Bowell, E., B. Hapke, D. Domingue, K. Lumme, J. Peltoniemi, and A. Harris 1989. Application of photometric model to asteroids. In *Asteroids II* (R. Binzel, T. Gehrels, and M. Matthews, Eds.), pp. 524–556. Univ. of Arizona Press, Tucson.

Danby, J. M. A. 1964. Stability of the triangular Lagrange points in the elliptic restricted problem of three bodies. *Astron. J.* **69**, 165–172.

Dunbar, R. S. 1980. *Dynamics and Stability of Trojan Librations in the Earth–Sun System: Implications for the Existence of an Earth Trojan Asteroid Group*. Ph.D. thesis, Princeton University.

Dunbar, R. S., and E. F. Helin 1983. Estimation of an upper limit on the Earth Trojan asteroid population from Schmidt survey plates. *Bull. Am. Astron. Soc.* **15**, 830.

Duncan, M., T. Quinn, and S. Tremaine 1989. The long-term evolution of orbits in the Solar System: A mapping approach. *Icarus* **82**, 402–418.

Mikkola, S., and K. Innanen 1990. Studies of Solar System dynamics II. The stability of Earth's Trojans. *Astron. J.* **100**, 290–293.

Mikkola, S., and K. Innanen 1995. On the stability of high inclination Trojans. *Earth Moon Planets* **71**, 195–198.

Murray, N., and M. Holman 1998. Diffusive chaos in the outer asteroid belt. *Astron. J.* **114**, 1246–1259.

Piironen, J., P. Magnusson, C. I. Lagerkvist, I. P. Williams, M. E. Buontempo, and L. V. Morrison 1997. Physical studies of asteroids. XXXI. Asteroid photometric observations with the Carlsberg Automatic Meridian Circle. *Astron. Astrophys. Suppl.* **121**, 489–497.

Pilcher, F. 1979. Circumstances of minor planet discovery. In *Asteroids* (T. Gehrels, Ed.), pp. 1130–1154. Univ. of Arizona Press, Tucson.

Rabinowitz, D. L. 1993. The size distribution of Earth-approaching asteroids. *Astrophys. J.* **407**, 412–427.

Rabinowitz, D. L. 1994. The size and shape of the near-Earth asteroid belt. *Icarus* **111**, 364–377.

Szebehely, V. 1967. *Theory of Orbits*. Academic Press, New York.

Weissman, P. R., and G. W. Wetherill 1974. Periodic Trojan-type orbits in the Earth–Sun system. *Astron. J.* **79**, 404–412.

Whiteley, R. J., and D. J. Tholen 1998. A CCD search for Lagrangian asteroids in the Earth–Sun system. *Icarus* **136**, 154–167.

Wiegert, P., K. Innanen, and S. Mikkola 1997. An asteroidal companion to the Earth. *Nature* **387**, 685–686.

Wisdom, J. 1980. The resonance overlap criterion and the onset of stochastic behavior in the restricted three body problem. *Astron. J.* **85**, 1122–1133.

Wisdom, J., and M. Holman 1991. Symplectic maps for the n-body problem. *Astron. J.* **102**, 2022–2029.